



NASA PO project NNX16AH60G
NASA Salinity projects 80NSSC20K0890

NSF NCAR-Wyoming Supercomputer Center

NOAA CVP grant
NA22OAR4310615-T1-01

Some thoughts on air-sea fluxes, large and small scale

Justin Small (NSF-NCAR),

Ian Grooms (CU)

Lucas Laurindo (UM)

Acknowledging: Frank Bryan,

Mike Alexander

Stu Bishop, Bob Tomas



CLIVAR PSMI panel Meeting July 23 2025

Overview

- Background (~historical) (Small)
 - Focus on turbulent heat fluxes (sensible and latent)
 - What drives the turbulent fluxes?
 - Large and small scale
 - What drives the SST?
 - Large and small-scale
 - Timescales
- Bulk fluxes and sub-grid scale variability (Grooms)
 - Parameterization ideas

A viewpoint from 1992...

Variability of Latent and Sensible Heat Fluxes Estimated Using Bulk Formulae

Daniel R. Cayan
Climate Research Division
Scripps Institution of Oceanography, 0224
La Jolla, CA 92093-0224

a Bulk Formulation of Latent and Sensible Fluxes

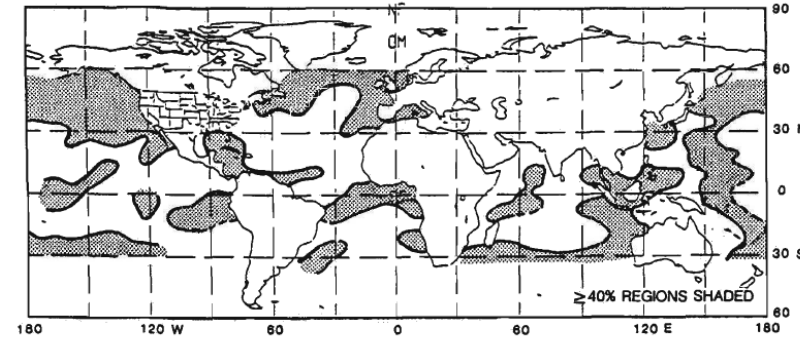
A form of the “sampling method” (Hanawa and Toba, 1987), employing the monthly average of the products of simultaneous observations ($w\Delta q$ and $w\Delta T$), is used to calculate the fluxes. (The COADS set does not provide the full heat flux formulation, but does furnish the $\{w\Delta q\}$ or $\{w\Delta T\}$ products averaged over simultaneous pairs of individual observations for each month.) The approximate form of the equations used here is

$$F_l = \rho L C_E \{w\Delta q\} \quad (3)$$

$$F_s = \rho C_p C_H \{w\Delta T\} \quad (4)$$

$$F_l' \approx \bar{w}\Delta q' + w'\bar{\Delta q}$$

Fraction of LHFLX variance due to Δq anomalies



Fraction of LHFLX variance due to wind anomalies

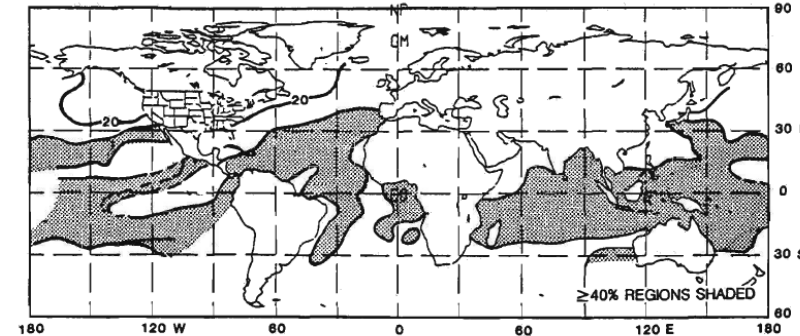


Fig. 7 Fraction (%) of F_l variance, $\sigma_{F_l}^2$, contributed by $\bar{w}^2 \Delta q'^2$ (above) and by $\Delta q'^2 \bar{w}^2$ (below); computed from December, January and February 1950–1986 data. Shading indicates regions with 40% of variance explained.

Based on marine surface observations – COADS ,
Woodruff et al. 1987. Monthly data.

Since our primary interest concerns air–sea interaction over several hundred kilometer scales, each of the COADS 2° data fields was averaged onto a 5° latitude–longitude grid, centered on 5° latitude–longitude intersections. The data density and the spatial averaging scheme is described in C1 and C2. For comparison

A viewpoint from 1992...

Latent and Sensible Heat Flux Anomalies over the Northern Oceans: Driving the Sea Surface Temperature

DANIEL R. CAYAN

Climate Research Division, Scripps Institution of Oceanography, La Jolla, California

(Manuscript received 27 December 1990, in final form 25 October 1991)

The bulk formulas for latent (F_l) and sensible (F_s) sea-air heat fluxes are

$$F_l = \rho L C_E w (q_s - q_a) \quad (1)$$

$$F_s = \rho C_p C_H w (SST - T_a), \quad (2)$$

where w , q_a , and T_a are the scalar wind (wind speed), specific humidity, and temperature of the air in the boundary layer at a given height (observation level)

$$\frac{\partial SST'}{\partial t} = -F' / \rho h C_p.$$

Correlation coefficient between SST tendency and turbulent heat fluxes

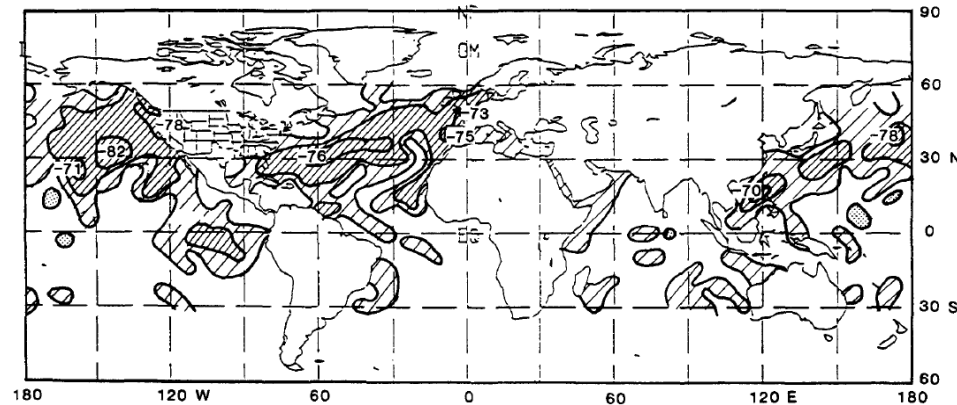


FIG. 2. Correlation coefficients ($\times 100$), mapped for global ocean F'_{ls} vs $\Delta SST' / \Delta t$ at each grid point, for winters 1946-86. Contours at 0, ± 0.3 , ± 0.5 , ± 0.7 . Light and heavy shading indicates correlations ≤ 0.3 and ≤ 0.5 . Hatching and stippling denote negative and positive correlations.

Based on marine surface observations – COADS, Woodruff et al. 1987. Monthly data.

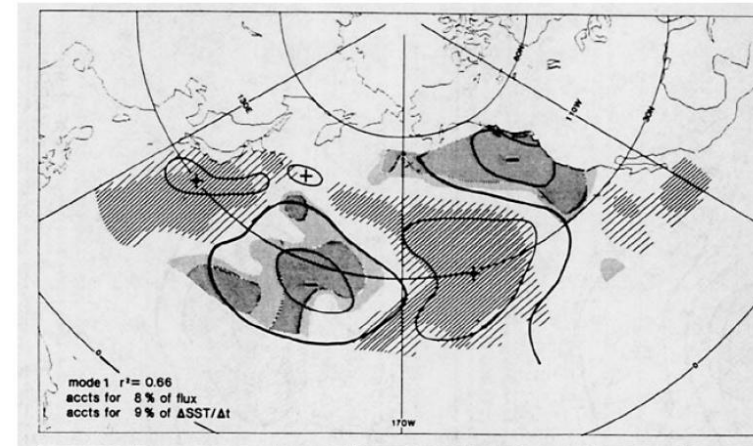


FIG. 4. Spatial patterns for the leading three North Pacific canonical correlation modes: g maps (solid lines), representing F'_{ls} patterns, vs h maps (shaded), representing $\Delta SST' / \Delta t$ patterns. Contours and shading show relative amplitude of the g and h maps, based on winter months of 1950-86. Positive/negative values of g maps are indicated by $+/-$ signs; positive/negative values of h maps are indicated by stippling/hatching.

PNA pattern

Since our primary interest concerns air-sea interaction over several hundred kilometer scales, each of the COADS 2° data fields was averaged onto a 5° latitude-longitude grid, centered on 5° latitude-longitude intersections. The data density and the spatial averaging scheme is described in C1 and C2. For comparison

A viewpoint from 1997...

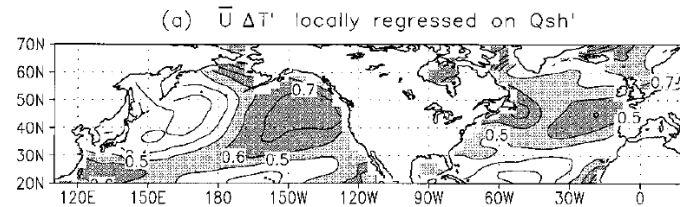
Surface Flux Variability over the North Pacific and North Atlantic Oceans

MICHAEL A. ALEXANDER AND JAMES D. SCOTT

CIRES, University of Colorado, Boulder, Colorado

(Manuscript received 22 January 1996, in final form 9 May 1997)

Regression: SHFLX due to ΔT anomalies



Regression: SHFLX due to wind anomalies

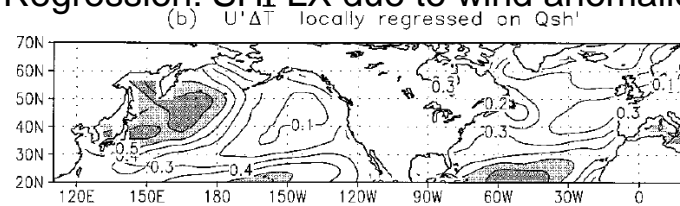
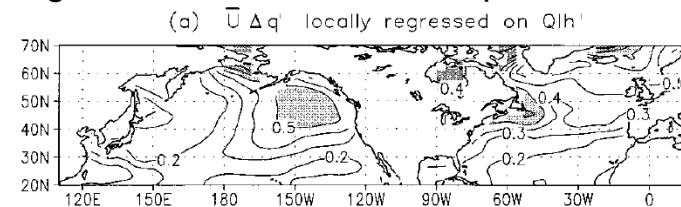


FIG. 11. Local regression values of $\rho c_p c_p$ times (a) $\bar{U} \Delta T'$ and (b) $U' \Delta T'$ on Q_{sh}' . The unitless values represent the fraction of Q_{sh}' related to the thermal and wind speed anomalies at that grid point. Contour interval is 0.1 and values between 0.5–0.6 are shaded light, while those greater than 0.6 are shaded dark.

Regression: LHFLX due to Δq anomalies



Regression: LHFLX due to wind anomalies

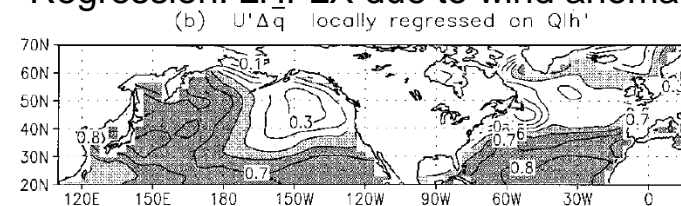


FIG. 12. Local regression values of $\rho c_p L$ times (a) $\bar{U} \Delta q'$ and (b) $U' \Delta q'$ on Q_{lh}' . The unitless values represent the fraction of Q_{lh}' related to (a) moisture and (b) wind speed anomalies at that grid point. Contour interval and shading as in Fig. 11.

Here we examine a 17-yr simulation performed with the Geophysical Fluid Dynamics Lab (GFDL) GCM, described in section 2, to examine the temporal and spatial variability of surface fluxes over the North Pa-

with storms. The SST and sea ice boundary conditions in the model simulation repeat the same seasonal cycle each year, thus we can isolate the surface flux variability, which is independent from oceanic fluctuations. In sec-

A viewpoint from 2003...

JOURNAL OF GEOPHYSICAL RESEARCH, VOL. 108, NO. C10, 3304, doi:10.1029/2002JC001750, 2003

TANIMOTO ET AL.: SST-HEAT FLUX RELATION

2 - 7

An active role of extratropical sea surface temperature in determining anomalous turbulent heat flux

Youichi Tanimoto,¹ Hisashi Nakamura,² Takashi Kagimoto, and Shozo Yama
Frontier Research System for Global Change, Yokohama, Japan

Received 18 February 2002; revised 23 April 2003; accepted 23 June 2003; published 1 October 2003.

Thus the anomalous fluxes at a particular instance at a given location can be expressed as follows:

$$\begin{aligned} Q'_E &= Q_E - \overline{Q_E} \\ &= \rho_a L C_E \{ \overline{U_a q'_s} - \overline{U_a q'_a} + U'_a (\overline{q_s} - \overline{q_a}) \\ &\quad + [U'_a (q'_s - q'_a) - \overline{U'_a (q'_s - q'_a)}] \} \end{aligned} \quad (6)$$

$$\begin{aligned} Q'_H &= Q_H - \overline{Q_H} \\ &= \rho_a c_p C_H \{ \overline{U_a T'_s} - \overline{U_a T'_a} + U'_a (\overline{T_s} - \overline{T_a}) \\ &\quad + [U'_a (T'_s - T'_a) - \overline{U'_a (T'_s - T'_a)}] \}. \end{aligned} \quad (7)$$

We focus on the first three terms of the right-hand side of equations (6) and (7) in the following analysis since the last two terms have indeed been found negligible. The first three terms of equation (7) are considered to represent the respective contributions from SSTA, SATA, and U'_a in this

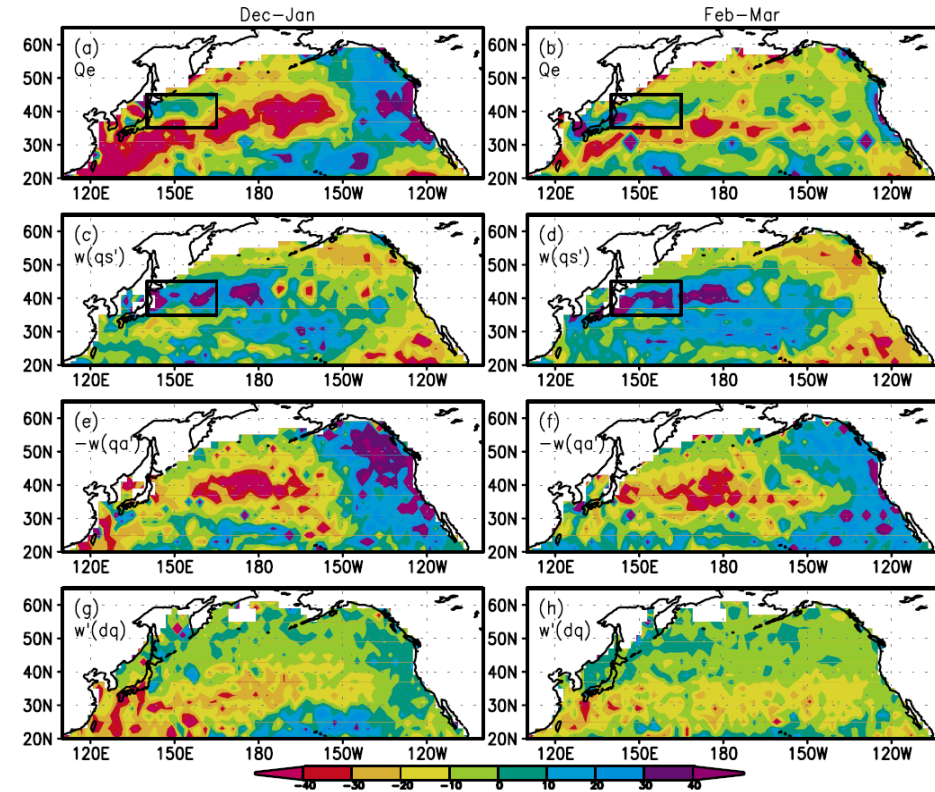


Figure 6. Same as in Figure 5, but for the (a, b) total upward latent heat flux anomalies, (c, d) SSTA contribution, (e, f) SATA contribution, and (g, h) scalar wind speed contribution to Figures 6a and 6b, respectively (unit: W m^{-2}). An inset rectangle in Figures 6a–6d indicates the domain $[35 \sim 45^\circ\text{N}, 140 \sim 165^\circ\text{E}]$, as in Figures 1c and 2c.

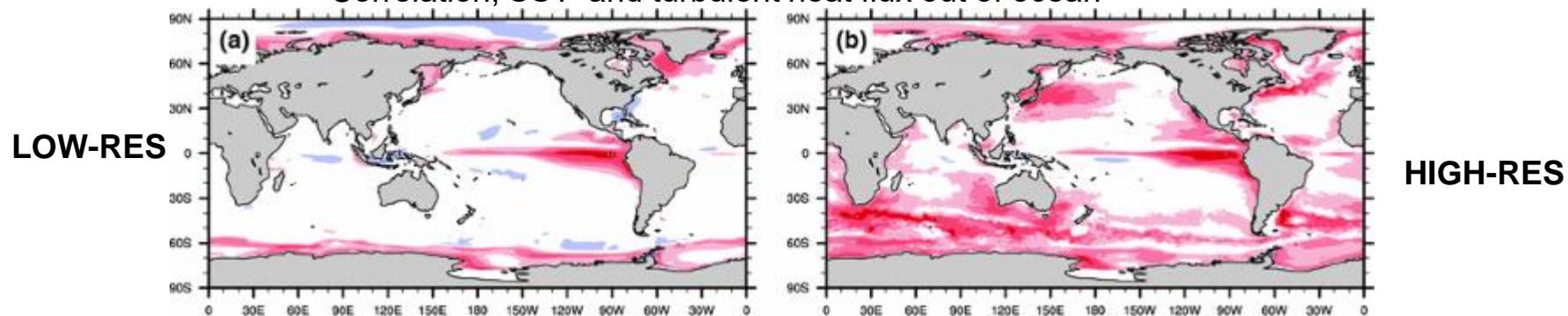
To represent the warm and cold phases of this wintertime decadal variability in the SAFZ, we selected a pair of 4-year periods; 1968/1969–1971/1972 winters (category DC+) and 1982/1983–1985/1986 winters (category DC–), based on Figure 3a of Nakamura *et al.* [1997a]. In Figure 4b, for the

A viewpoint from 2012...

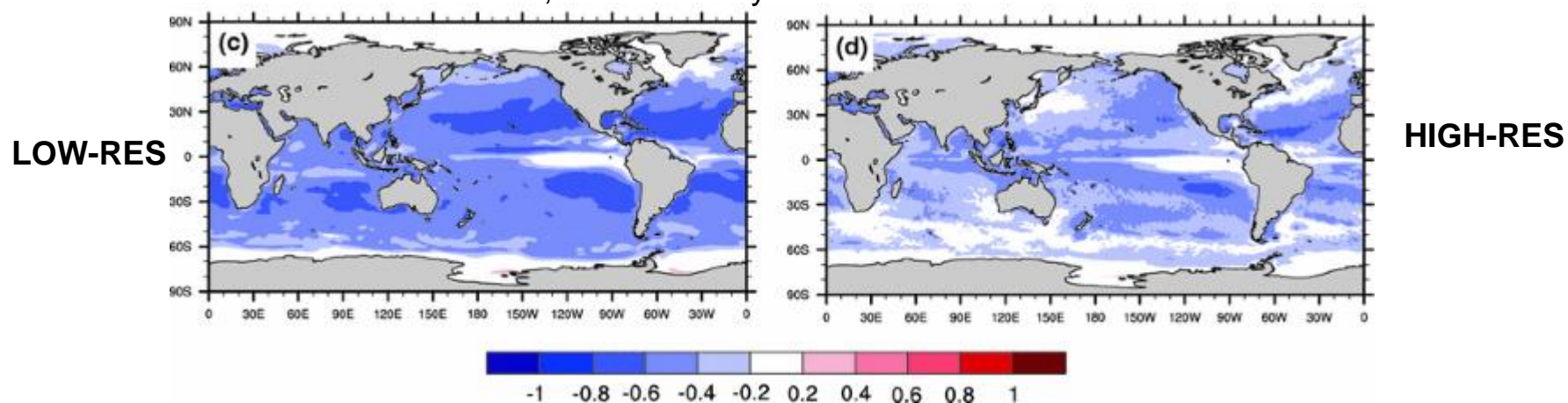
Impact of ocean model resolution on CCSM climate simulations

Ben P. Kirtman · Cecilia Bitz · Frank Bryan · William Collins · John Dennis ·
Nathan Hearn · James L. Kinter III · Richard Loft · Clement Rousset ·
Leo Siqueira · Cristiana Stan · Robert Tomas · Mariana Vertenstein

Correlation, SST' and turbulent heat flux out of ocean

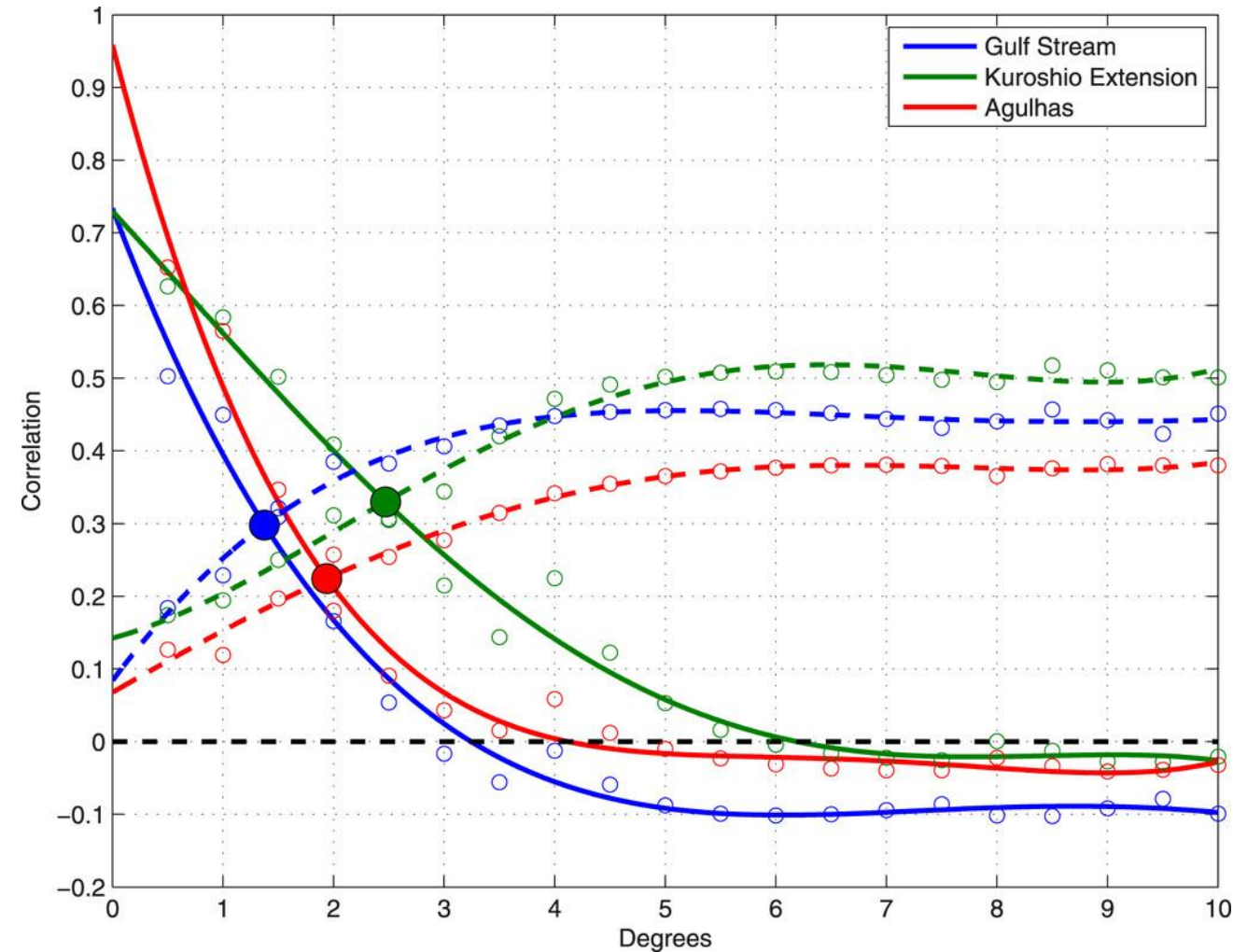


Correlation, SST tendency and turbulent heat flux out of ocean



A viewpoint from 2017...

OAFLUX



Scale Dependence of Midlatitude Air–Sea Interaction

STUART P. BISHOP

North Carolina State University, Raleigh, North Carolina

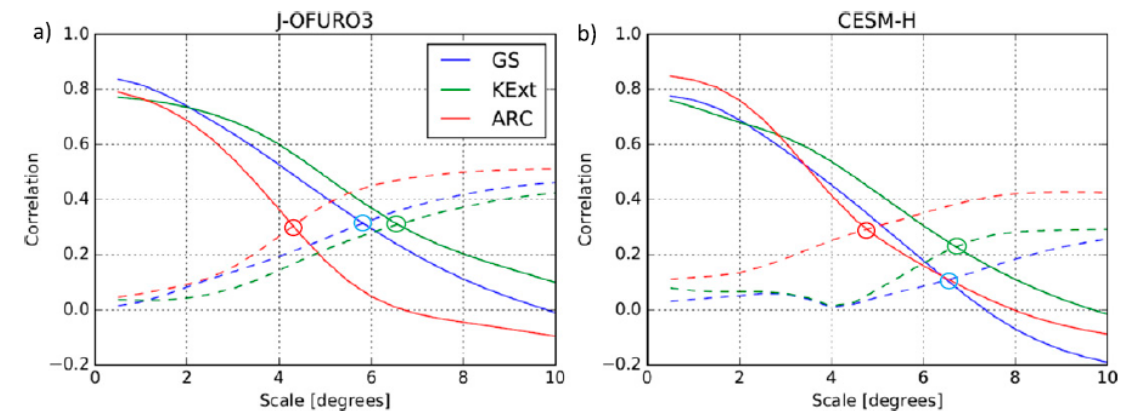
R. JUSTIN SMALL, FRANK O. BRYAN, AND ROBERT A. TOMAS

National Center for Atmospheric Research, Boulder, Colorado

(Manuscript received 9 March 2017, in final form 30 June 2017)

Method for determining the transition length scale L_c . Solid curves are best fit to r_{T0} and dashed curves are best fit to r_{T0} at monthly time scales as a function of space scale δ_c at the WBC locations in Fig. 10. Open circles are the raw data, and larger colored circles are the intersection locations

Updated in Small et al. 2019





A viewpoint from 2019...

Air–Sea Turbulent Heat Fluxes in Climate Models and Observational Analyses: What Drives Their Variability?

R. JUSTIN SMALL AND FRANK O. BRYAN

National Center for Atmospheric Research, Boulder, Colorado

STUART P. BISHOP

North Carolina State University, Raleigh, North Carolina

ROBERT A. TOMAS

National Center for Atmospheric Research, Boulder, Colorado

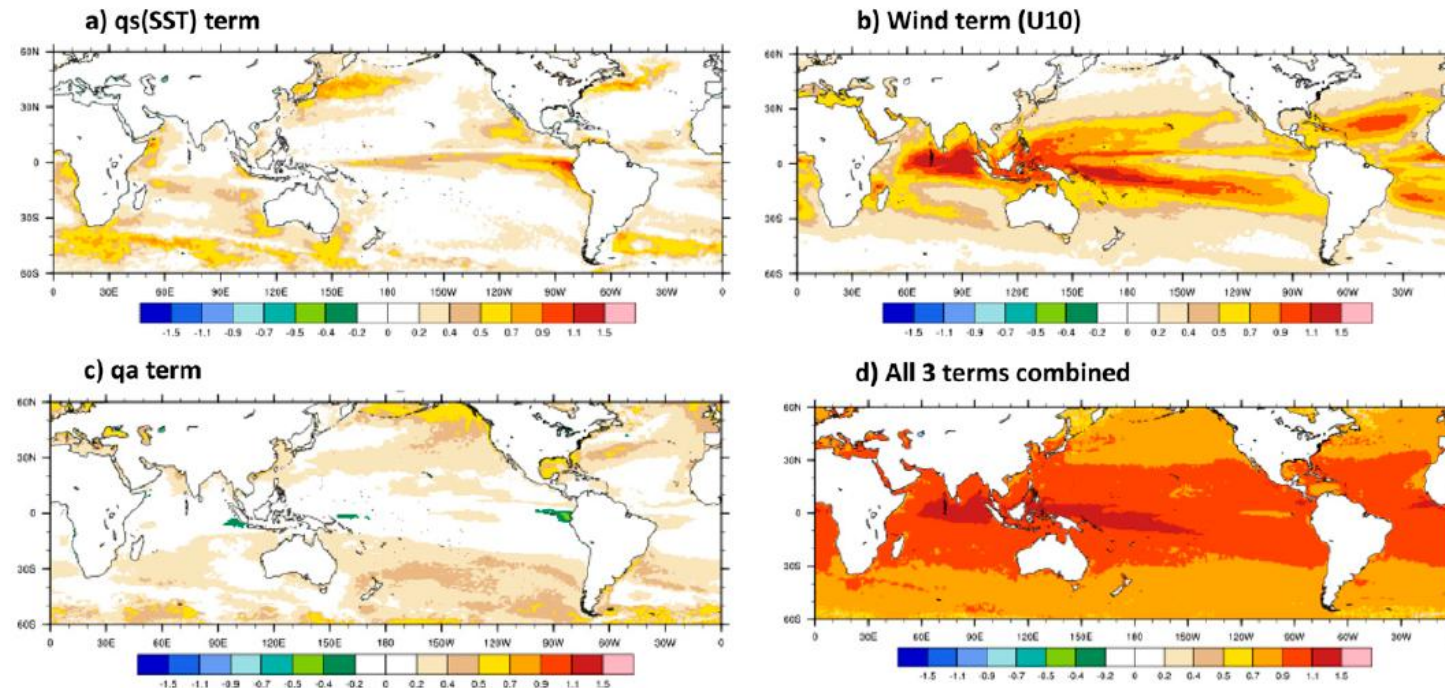
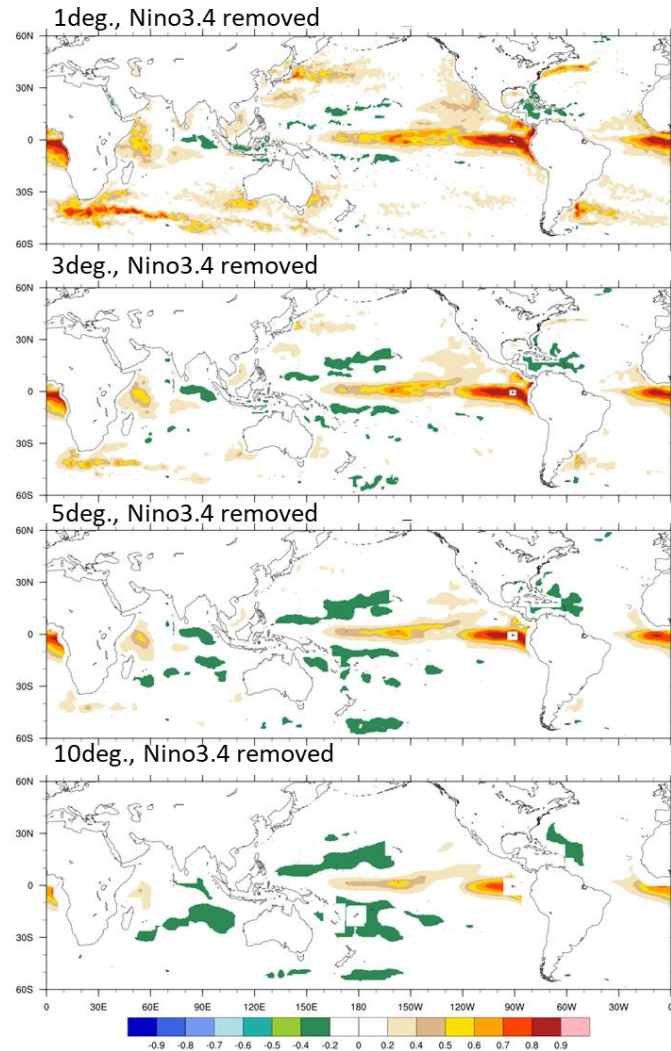


FIG. 11. Linear regression of individual terms of LHF decomposition onto full LHF variability, based on CESM-HR, from method 2: (a) q_s (SST) contribution, (b) wind contribution, (c) air humidity contribution, and (d) contribution of all three terms. The displayed quantity is unitless.

Air-Sea Turbulent Heat Fluxes in Climate Models and Observational Analyses: What Drives Their Variability?

Correlations between SST and turbulent heat flux

Sensitivity to spatial scale



Sensitivity to time scale

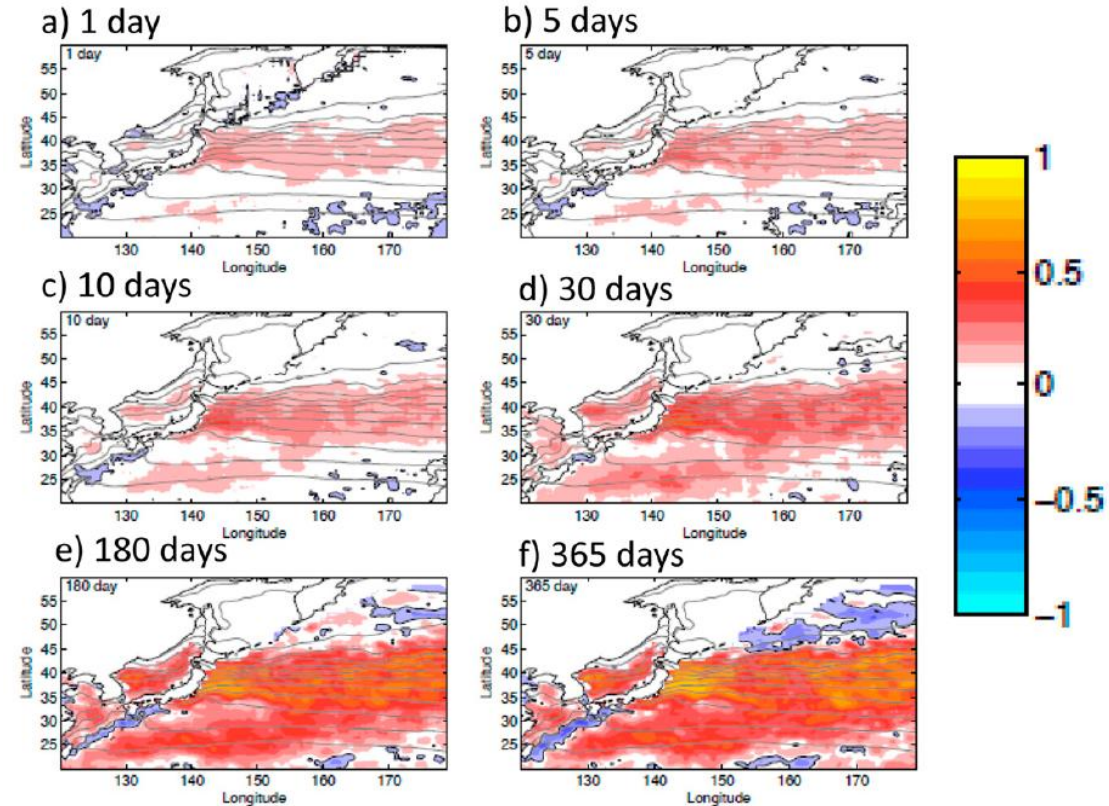


FIG. 15. The correlation of SST and turbulent heat flux in the northwest Pacific for different time scales. Data are from the OAFlux (Yu and Weller 2007) product. The data are low-pass filtered for the number of days labeled at the top of each plot (see text for details). The climatological annual cycle is removed, as is regression on Niño-3.4 SST.

A viewpoint from 2022...

JGR Oceans












RESEARCH ARTICLE

10.1029/2021JC018340

Role of Ocean and Atmosphere Variability in Scale-Dependent Thermodynamic Air-Sea Interactions

Special Section:

Community Earth System
Model High-Resolution
(CESM-HR) Special Collection

Lucas C. Laurindo^{1,2} , R. Justin Small^{1,2} , LuAnne Thompson³ , Leo Siqueira⁴ ,
Frank O. Bryan² , Ping Chang^{1,5,6} , Gokhan Danabasoglu^{1,2} , Igor V. Kamenkovich⁴ ,
Ben P. Kirtman⁴ , Hong Wang^{1,7,8} , and Shaoqing Zhang^{1,7,8} 

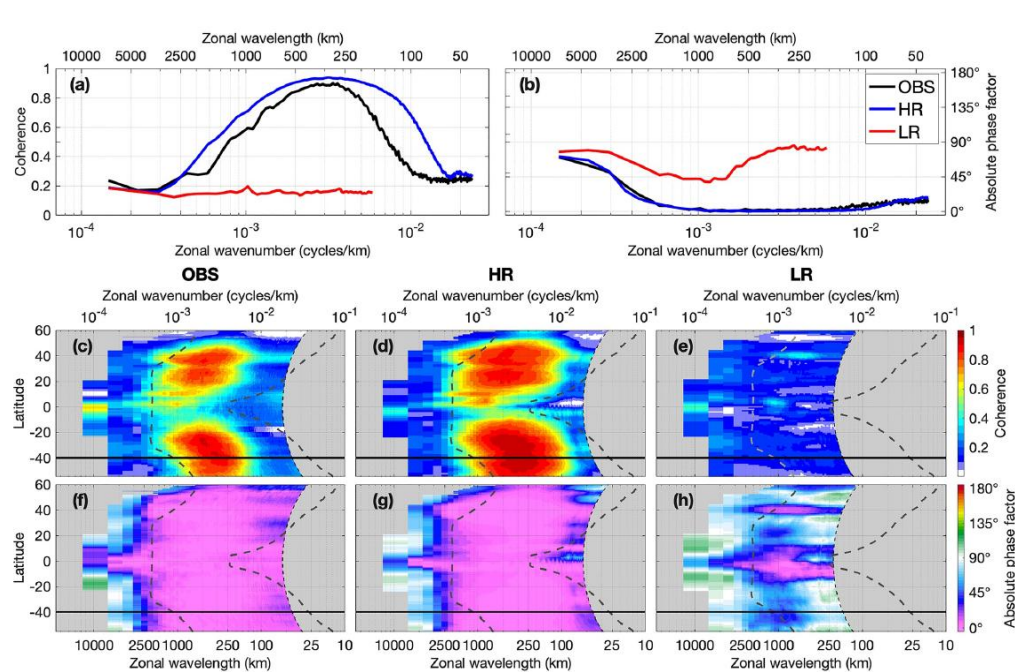


Figure 4. Coherence (γ_{TQ}^2) and absolute phase factor (θ_{TQ}) between sea surface temperature (SST) and turbulent heat flux (THF) in zonal wavenumber domain for the Pacific Ocean resolved by high-resolution (HR), low-resolution (LR), and satellite observations (OBS). The top row (a–b) exemplify estimates for 40°S while the middle (c–e) and bottom (f–h) rows show latitudinal spectrograms. The left and right thick dashed lines in (c–h) represent the zonally-averaged first internal Rossby radius of deformation for the atmosphere and the ocean, respectively; the thin black dashed denotes the spatial Nyquist frequency for the spectral analysis; and the black horizontal line marks the 40°S latitude that the estimates in panels (a–b) refer to.

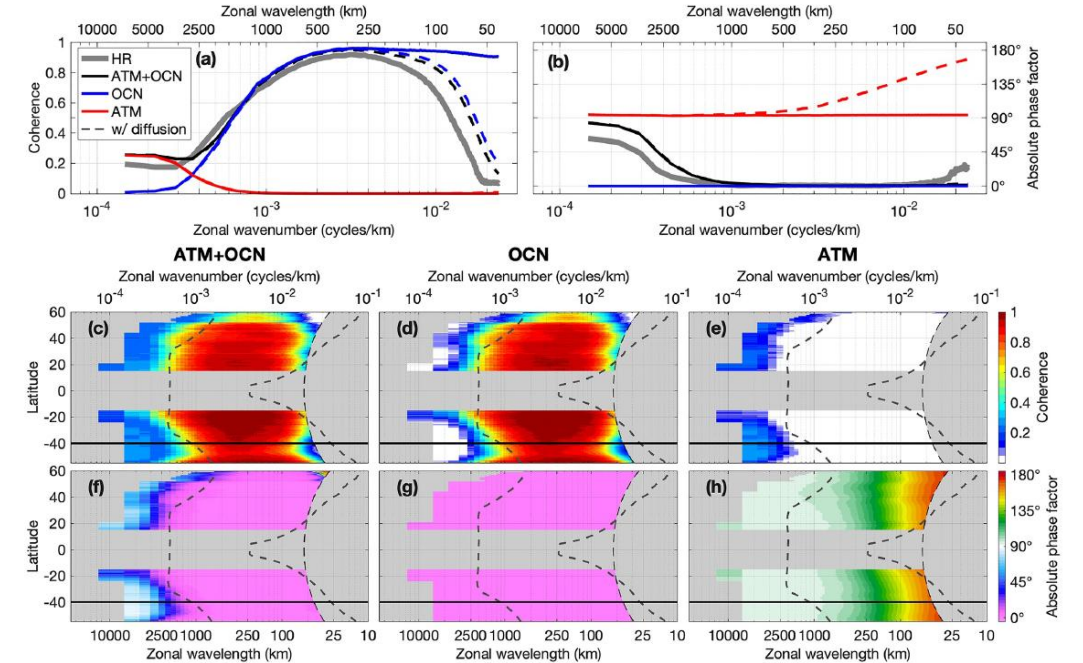


Figure 6. Stochastic model estimates of the coherence (γ_{TQ}^2) and absolute phase factor (θ_{TQ}) between sea surface temperature (SST) and turbulent heat flux (THF) as a function of zonal wavenumber (k) for high-resolution (HR). The top row (a–b) exemplifies the ocean and atmosphere-driven components of the stochastic model solutions (ocean-driven [OCN], blue and red lines, respectively), their sum (ATM + OCN, black), and the reference estimates from the HR simulations (thick gray line). The middle (c–e) and bottom (f–h) rows are latitudinal spectrograms of the ATM + OCN, OCN, and ATM components of γ_{TQ}^2 and θ_{TQ} , respectively. The left and right dashed lines in (c–h) represent the zonally-averaged first internal Rossby radius of deformation for the atmosphere and the ocean, respectively, the thin dashed line is the spatial Nyquist frequency for the spectral analysis, and the black horizontal line marks the 40°S latitude used to plot the results in (a–b).

Near-Surface Atmospheric Response to Meso- and Submesoscale Current and Thermal Feedbacks

CARLOS CONEJERO,^a LIONEL RENAULT,^a FABIEN DESBIOLLES,^{b,c} J. C. MCWILLIAMS,^d AND HERVÉ GIORDANI^e

^a *Université de Toulouse, LEGOS (CNES/CNRS/IRD/UT3), Toulouse, France*

^b *Department of Earth and Environmental Sciences, Università di Milano-Bicocca, Milan, Italy*

^c *CIMA Research Foundation, Savona, Italy*

^d *Department of Atmospheric and Oceanic Sciences, University of California, Los Angeles, Los Angeles, California*

^e *Météo-France, Toulouse, France*

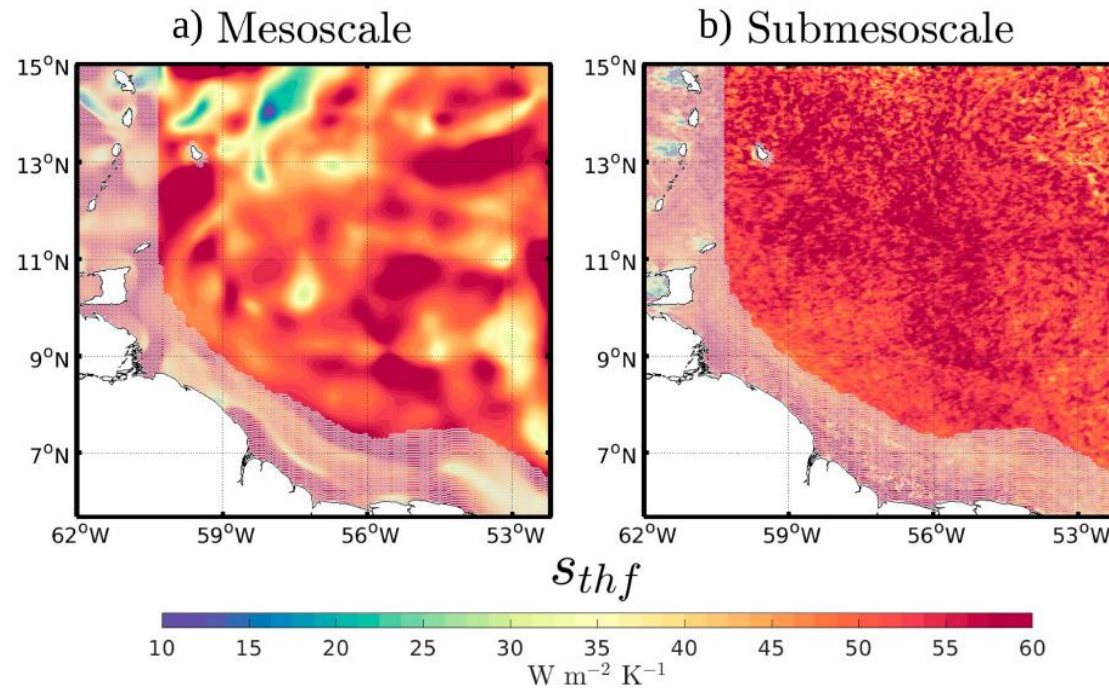


FIG. 10. Coupling coefficient between the surface turbulent heat flux and SST anomalies s_{thf} (see section 2): (a) spatial distribution of mesoscale s_{thf} , (b) spatial distribution of submesoscale s_{thf} , and (c) binned scatterplot of the surface

Some thoughts

- Biases in the state variables are still important for climate models and reanalysis (e.g. recent findings by Frank Bryan, Elizabeth Thompson)
- Requirements for observations, e.g. Cronin et al. 2019 suggestions, saildrones,...
- Now we are moving to even smaller scales – limitation of bulk flux assumptions, model grid size
 - How to treat sub-grid scale variability (following slides)

Proposed parameterization strategy, NOAA 2022

Consider the air-sea momentum flux averaged over a coarse grid cell

$$\bar{\tau} = \bar{\tau}(T_a, T_s, U_a, U_s, \dots) = \tau(\overline{T_a} + T'_a, \overline{T_s} + T'_s, \overline{U_a} + U'_a, \overline{U_s} + U'_s, \dots)$$

In a coarse model we don't know the subgrid perturbations, so we instead use

$$\bar{\tau} \approx \tau(\overline{T_a}, \overline{T_s}, \overline{U_a}, \overline{U_s}, \dots)$$

We proposed improve this by generating N synthetic, stochastic samples from a joint subgrid-scale distribution and then averaging them:

$$\bar{\tau} \approx \frac{1}{N} \sum_{n=1}^N \tau(\overline{T_a} + T_a^{(n)}, \overline{T_s} + T_s^{(n)}, \overline{U_a} + U_a^{(n)}, \overline{U_s} + U_s^{(n)}, \dots)$$

Proposed parameterization strategy, NOAA 2022

An easily-implementable preliminary approach motivated by Brankart (Ocean Modelling, 2013) is to simulate N random walks around each grid cell, sampling the local atmospheric and oceanic spatial variability.

A more accurate approach would be to use a combination of physical insight and high-resolution coupled data to learn the joint distribution of SGS variables as a function of large-scale input variables – a physics-informed generative-modeling ML approach – and sample from that. Both approaches could be used in combination with improved bulk formulae.



Ocean Modelling
Volume 66, June 2013, Pages 64-76



Impact of uncertainties in the horizontal
density gradient upon low resolution global
ocean modelling

Jean-Michel Brankart ✉